Pergamon

Geochimica et Cosmochimica Acta, Vol. 60, No. 18, pp. 3375–3381, 1996

0016-7037/96 $15.00 + .00

PII S0016-7037(96)00181-0

# The kinetics of the reaction $CO_2 + H_2O \rightarrow H^+ + HCO_3^-$ as one of the rate limiting steps for the dissolution of calcite in the system $H_2O-CO_2-CaCO_3$

W. DREYBRODT, J. LAUCKNER, LIU ZAIHUA, U. SVENSSON, and D. BUHMANN
Institute of Experimental Physics, University of Bremen, D-28334 Bremen, Germany

(*Received October* 19, 1995; *accepted in revised form May* 20, 1996)

**Abstract**—Dissolution of $CaCO_3$ in the system $H_2O$-$CO_2$-$CaCO_3$ is controlled by three rate-determining processes: The kinetics of dissolution at the mineral surface, mass transport by diffusion, and the slow kinetics of the reaction $H_2O + CO_2 = H^+ + HCO_3^-$. A theoretical model of Buhmann and Dreybrodt (1985a,b) predicts that the dissolution rates depend critically on the ratio $V/A$ of the volume $V$ of the solution and the surface area $A$ of the reacting mineral. Experimental data verifying these predictions for stagnant solutions have been already obtained in the range 0.01 cm $< V/A <$ 0.1 cm. We have performed measurements of dissolution rates in a porous medium of sized $CaCO_3$ particles for $V/A$ in the range of $2 \cdot 10^{-4}$ cm and 0.01 cm in a system closed with respect to $CO_2$ using solutions pre-equilibrated with an initial partial pressure of $CO_2$ of $1 \cdot 10^{-2}$ and $5 \cdot 10^{-2}$ atm. The results are in satisfactory agreement with the theoretical predictions and show that especially for $V/A < 10^{-3}$ cm dissolution is controlled entirely by conversion of $CO_2$ into $H^+$ and $HCO_3^-$, whereas in the range from $10^{-3}$ cm up to $10^{-1}$ cm both $CO_2$-conversion and molecular diffusion are the rate controlling processes. This is corroborated by performing dissolution experiments using 0.6 $\mu$molar solutions of carbonic anhydrase, an enzyme enhancing the $CO_2$-conversion rates by several orders of magnitude. In these experiments $CO_2$ conversion is no longer rate limiting and consequently the dissolution rates of $CaCO_3$ increase significantly. We have also performed batch experiments at various initial pressures of $CO_2$ by stirring sized calcite particles in a solution with $V/A$ = 0.6 cm and $V/A$ = 0.038 cm. These data also clearly show the influence of $CO_2$-conversion on the dissolution rates. In all experiments inhibition of dissolution occurs close to equilibrium. Therefore, the theoretical predictions are valid for concentrations $c \leq 0.9\ c_{eq}$. Summarising we find good agreement between experimental and theoretically predicted dissolution rates. Therefore, the theoretical model can be used with confidence to find reliable dissolution rates from the chemical composition of a solution for a wide field of geological applications.

## 1. INTRODUCTION

The conversion of $CO_2$ into $H^+$ and $HCO_3^-$-ions in an aqueous solution is an important chemical reaction in many geological processes, such as $CO_2$-transfer across air-water interfaces (House and Howard, 1984), chemical weathering of rocks, and especially dissolution and precipitation of carbonate minerals, e.g., limestone and dolomite (Buhmann and Dreybrodt, 1985a,b; Dreybrodt and Buhmann, 1991; Dreybrodt et al., 1992; Dreybrodt 1988; Liu Zaihua et al., 1995). Two parallel reactions control this process (Kern, 1960; Usdowski, 1982; Stumm and Morgan, 1981),

$$CO_2 + H_2O \leftrightharpoons H_2CO_3 \leftrightharpoons H^+ + HCO_3^-, \quad \text{(I)}$$

$$CO_2 + H_2O \leftrightharpoons CO_2 + H^+ + OH^- \leftrightharpoons H^+ + HCO_3^-. \quad \text{(II)}$$

The hydration of $CO_2$ in reaction I is slow, whereas the dissociation of carbonic acid is so fast that in practically all cases $H_2CO_3$,$H^+$ and $HCO_3^-$ are in equilibrium. The forward rate constant of the total reaction I is $k_{CO_2} = 3 \cdot 10^{-2} s^{-1}$ and the constant $k_{H_2CO_3}$ of the backward reaction is 12 $s^{-1}$ at 25°C. Reaction II becomes dominant at high pH (>9). Its forward rate constant is $k_+ = 8.5 \cdot 10^{-3}$ mole$^{-1}$s$^{-1}$, the back reaction constant is $k = 2 \cdot 10^{-4} s^{-1}$ at 25°C. For illustration, a solution of initially $10^{-5}$ mole $CO_2$ in pure water attains equilibrium within 20 s at 25°C (Stumm and Morgan, 1981). Usdowski (1982) has reported reaction times in buffered calcareous solutions with fixed pH ranging from 6–9 at 25°C. Such solutions are characteristic for groundwaters of the type $Ca^{2+} - Mg^{2+} - HCO_3^-$, as they occur in limestone terrains. At 25°C, 99% of equilibrium of $CO_2$ is attained in about 100 s for pH-values between 7 and 9. These examples show that for most groundwaters, $CO_2$-conversion is a slow reaction.

Dissolution of calcite in $CO_2$-containing water plays an important role in many geological processes. The sculpturing of karst landscapes and caves in limestone terrains are probably the most spectacular ones. (Trudgill, 1985; Ford and Williams, 1989; White, 1988). To understand the evolution of such landscapes the knowledge of the chemical kinetics of calcite dissolution is of utmost importance (Dreybrodt, 1988, 1990; Palmer 1984, 1991). Since dissolution of calcite is determined by the overall reaction $CaCO_3 + CO_2 + H_2O \leftrightharpoons Ca^{2+} + 2HCO_3^-$ stochiometry requires that for each $Ca^{2+}$ released into the solution one molecule of $CO_2$ has to be converted into $HCO_3^-$ and $H^+$. Therefore, during dissolution of calcite with a surface $A$ by water of volume $V$ the following relation holds

$$V \cdot \frac{d[CO_2]}{dt} = AR, \quad (1)$$

where $[CO_2]$ is the concentration of $CO_2$ and $R$ is the flux of $Ca^{2+}$ from the mineral surface. $R$ depends on the chemical composition of the solution. In their pioneering work, Plummer et al. (1978) suggested a rate law for $R$, called the PWP-equation later on, given by

$$R = \kappa_1(H^+) + \kappa_2(H_2CO_3^*) + \kappa_3 - \kappa_4(Ca^{++})(HCO_3^-), \quad (2)$$

where $\kappa_1$, $\kappa_2$, and $\kappa_3$ are temperature dependent rate constants, and $\kappa_4$ is a rate constant, which depends also on $(H_2CO_3^*)$. The round brackets denote activities of the corresponding species at the surface of the mineral. $R$ is measured in units of mole $cm^{-2}$ $s^{-1}$. From Eqns. 1 and 2 follows immediately that for small values of $V/A$ the conversion of $CO_2$ can be rate limiting. If, however, the volume of the solution becomes so large that the amount of $CO_2$ consumed during the dissolution is not sufficient to change its concentration, then the surface reaction or mass transport determines the dissolution rates. Therefore, the kinetics of $CO_2$-conversion becomes important in all geological processes, where large areas of mineral surfaces are in contact with small volumes of water. Such situations arise during diagenesis in sediments where dissolution and precipitation of calcite play an important role, and also in the initiation of karst aquifers, where narrow fractures of about $10^{-2}$ cm are widened by calcite aggressive solutions, flowing through them. Hydraulic structures, such as dams, built in limestone terrains, may be endangered by enhanced widening of narrow fractures beneath them (Palmer, 1988; Dreybrodt, 1992; James, 1992) and reliable data on calcite dissolution kinetics are necessary for safety estimations. Dissolution and precipitation of calcite by water layers in contact with the mineral surface have been investigated theoretically by Buhmann and Dreybrodt (1985a,b, 1987) and by Dreybrodt and Buhmann (1991). These authors verified their theoretical model by experiments with $V/A$-ratios from 0.03–0.1 cm. Baumann et al. (1985) and Schulz (1988) extended this work to the dissolution kinetics in porous media. Their experimental data show that the theoretical predictions of the model are also valid for porous media with grain sizes from 0.05 cm up to 0.2 cm. Since, however, the influence of $CO_2$-conversion as a rate limiting process increases with decreasing volume, i.e., decreasing pore size experimental data are needed for grain sizes down to $10^{-3}$ cm. Therefore, to cover the full range of the theoretical model, more experimental data are necessary. These are provided in this work.

## 2. THEORETICAL BACKGROUND

Two system conditions can be defined for dissolution or precipitation of calcite. If the solution is in contact with a $CO_2$-containing atmosphere, there will be a flux of $CO_2$ into the solution (open-system). If this, however, is not the case, $CO_2$ will be consumed and its concentration drops (closed-system). In the following we will deal with the latter, since all experiments were performed in a system closed to the uptake of $CO_2$.

To obtain dissolution rates for the system $H_2O$-$CO_2$-$CaCO_3$, one has to solve a set of transport equations, which contain (a) diffusional mass transport of the dissolved ionic species $Ca^{2+}$, $HCO_3^-$, and $CO_3^{2-}$ from the mineral surface, and mass transport of the reactant species $CO_2$, $H_2CO_3$, and $H^+$ towards it; (b) the kinetics of $CO_2$-conversion (cf. reaction I, II); and (c) the surface kinetics expressed by Eqn. 2 as a boundary condition (Buhmann and Dreybrodt, 1985a,b). The results of such calculations are illustrated by

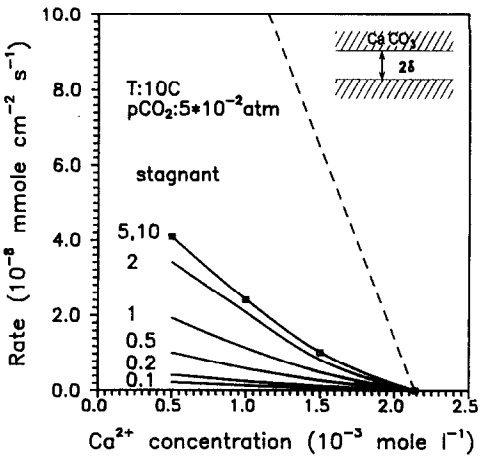


FIG. 1. Dissolution rates from the theoretical model for a free drift run under the conditions of a system closed to $CO_2$. The numbers on the curves denote the value of $\delta$, i.e., half the distance between the parallel calcite surfaces in $10^{-3}$ cm. For $\delta = 5 \cdot 10^{-3}$ cm and $\delta = 1 \cdot 10^{-2}$ cm the curves are identical. This is shown by the open squares which correspond to $\delta = 1 \cdot 10^{-2}$. The dashed curve gives the rates for turbulent motion and $\delta = 1$ cm. The insert in the upper right depicts the geometry of the model.

Fig. 1. It depicts the dissolutional rates as a function of the $Ca^{2+}$-concentration, which has been accumulated during a free drift run under closed-system conditions, with an initial $CO_2$-concentration in equilibrium with a $p_{CO_2} = 5 \cdot 10^{-2}$ atm fora stagnant solution contained between two parallel planes with distance $2\delta$. The numbers on the curves denote the values of $\delta$ in $10^{-3}$ cm.

At small values of $\delta \leq 2 \cdot 10^{-3}$ cm the rates increase proportionally to $\delta$. This is the region where conversion of $CO_2$ is rate limiting. For values between $0.002 \leq \delta \leq 0.1$ cm the rates become independent of $\delta$. In this case both molecular diffusion and $CO_2$-conversion determine the rates due to chemically enhanced diffusion. The upmost dashed curve was calculated for a completely mixed solution where concentration gradients are avoided by increasing the constant of molecular diffusion by a factor of $10^4$. Furthermore, $\delta = 1$ cm. This simulates turbulent motion in the water, where mass transport is enhanced such that it is no longer rate limiting. Furthermore, due to the large value of $\delta$, $CO_2$-conversion is no longer rate limiting either. The large increase of the rates under these conditions in comparison to values of $\delta < 0.1$ cm stresses the importance of molecular diffusion and $CO_2$-conversion as rate limiting mechanisms. The importance of $CO_2$-conversion is also illustrated by Fig. 2, which differs from Fig. 1 in that turbulence in the solution enhances mass transport in all cases. The influence of $CO_2$ is clearly seen. At small values of $\delta$ between $5 \cdot 10^{-4}$ and $5 \cdot 10^{-3}$ cm the rates increase linearly with $\delta$. At large volumes, $V/A = \delta \geq 0.1$ cm, however, no further increase of the rates is found, since $CO_2$-conversion is no longer rate limiting. We will come back to these figures, when interpreting the experimental data. It should be noted here that the results shown by Fig. 1 remain also valid if one considers a porous medium with stagnant fluid and replaces $\delta$ by the volume/surface ratio $V/A$. (Baumann et al., 1985; Schulz, 1988). The results of Fig. 2 remain also valid for batch

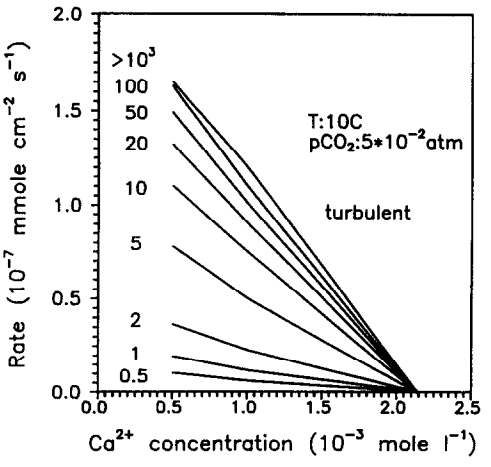


FIG. 2. Dissolution rates as in Fig. 1. But now the water is in turbulent motion. This has been simulated by replacing the coefficient of molecular diffusion $D_m$ by an effective eddy diffusion coefficient $D_{eff} = 10^4 \cdot D_m$. Numbers on curves denote $\delta$ in $10^{-3}$ cm.

experiments, where calcite particles with total surface $A$ are stirred turbulently in a solution with volume $V$. The reason for this is that turbulent motion establishes perfect mixing and excludes any gradients in concentrations. All the curves in Figs. 1 and 2 can be approximated by a linear relation

$$R = \alpha(c_{eq} - c), \tag{3}$$

where $\alpha$ is the kinetic constant in cm s$^{-1}$, and $c$, $c_{eq}$ are the actual and the equilibrium calcium concentrations in mole cm$^{-3}$, respectively. Values of $\alpha$ are tabulated for a variety of temperatures and partial pressures of $CO_2$ by Buhmann and Dreybrodt (1985a,b, 1987, 1988). The values of $\alpha$ depend on temperature, the partial pressure of $CO_2$ in equilibrium with the solution, and the $V/A$-ratio. They furthermore depend on the reaction path in that they differ for closed- and open-system conditions. Finally, the hydrodynamics of the solution plays an important role. Turbulently flowing solutions under otherwise identical conditions exhibit higher values of $\alpha$ than laminar flowing or stagnant solutions. It is, therefore, not possible to give simple empirical relations for $\alpha$. In each case one has to use the computer program. This program can be obtained on request by W. Dreybrodt.

## 3. EXPERIMENTAL METHODS

### 3.1. Samples and Sample Preparation

Baker Analyzed Reagent $CaCO_3$ was prepared by suspending it in bidistilled water to remove microparticles. Then the material was treated for 10 s with diluted HCl and washed with bidistilled water. The material was stored after drying at 50°C for 5 h. A microscopic analysis revealed crystals of an average size of 15 $\mu$m, which yields a geometric surface area of 1740 cm$^2$/g, similar to the area of 1840 cm$^2$/g obtained by BET-measurements.

Natural marble (Naxos, Greece) was broken down and sized by wet sieving with deionized water to fractions between 90 $\mu$m and 120 $\mu$m, 120 $\mu$m and 180 $\mu$m, 250 $\mu$m and 350 $\mu$m, 350 $\mu$m and 550 $\mu$m, and 700 $\mu$m and 1000 $\mu$m. The samples were treated with diluted HCl (0.01 molar) for 10 s, rinsed in bidistilled water and finally with acetone. Then they were dried and stored for further use. Carbonic anhydrase was purchased as lyophilized powder from SIGMA and used as obtained.

### 3.2. Apparatus

The first type of experiments has been carried out as batch runs, using the free-drift-technique, where synthetic calcite was kept in suspension by turbulently stirring the solution with a propeller at 320 rpm. Figure 3 shows the experimental set-up. The solution is contained in a Teflon vessel with a volume of 262 cm$^3$, such that no further space is available for air. The vessel is sealed to be airtight. The experiment is started by filling the vessel with a solution of $CO_2$ in distilled water in equilibrium with a $CO_2$-$N_2$-atmosphere with a $CO_2$ partial pressure of $5 \cdot 10^{-3}$, $1 \cdot 10^{-2}$, or $1 \cdot 10^{-1}$ atm. The temperature of the solution was kept constant to 20° ± 0.1 C during the whole experiment. Immediately after filling a given amount of $CaCO_3$ (4 g or 0.25 g) was introduced, the vessel was sealed by a stopper and the stirrer was switched on. The increase in calcium concentration was monitored by measuring the conductivity of the solution. At the end of the run the solution was analysed for its calcium concentration $c$ as a gauge for the conductivity. Since in all experiments maximal ionic strength was $I_{max} = 0.009$, all solutions are sufficiently diluted to exhibit a linear relation between conductivity and $Ca^{++}$-concentration. The concentration of ionic pairs is less than 2% of the Ca-concentration. This was checked by calculating the chemical composition of the solution with respect to $Ca^{2+}$, $HCO_3^-$, $CO_3^{--}$, and $H^+$ by the program equilibrium (Dreybrodt, 1988) for closed pathways as used in the experiments. Using the thus obtained concentrations we employed the program WATEQ4F to calculate the conductivity and the concentration of ionic pairs. We found a linear relation $c = 5.35\ \sigma - 5.27 \cdot 10^{-2}$, where $c$ is in mmole/$\ell$ and the conductivity $\sigma$ in $\mu$s/cm. This is close to the empirical relation (Langmuir, 1971) for carbonate groundwater. The concentration of the ion pairs turned out to be negligible.

The dissolution rates were calculated by the relation

$$\frac{V}{A}\frac{dc(t)}{dt} = R. \tag{4}$$

Before the numerical differentiation, the $c(t)$-course was smoothed by a 4 point averaging procedure to avoid too large noise in the time derivative.

The second type of experiments employed dissolution of calcite from a porous medium with a stagnant solution contained in it. The experimental set up is shown in Fig. 4. The upper drawing represents a longitudinal section of the set up. A WTW-conductivity cell (Tetracon LF 325) (1), also shown in top view below, is surrounded by a cooling vessel (5) to keep the temperature constant to ±0.1°C.

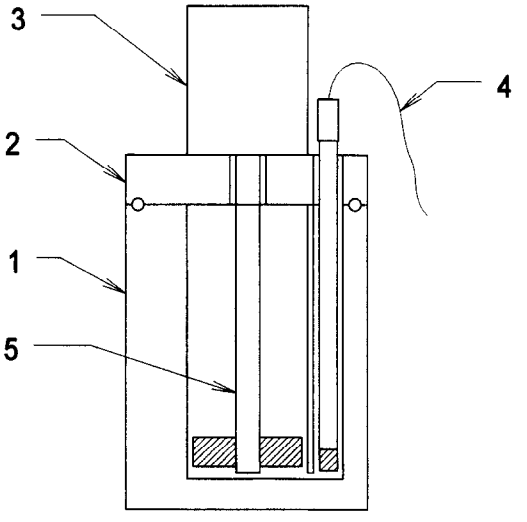


FIG. 3. Experimental set up for a batch run. A vessel of Teflon (1) is sealed by a lid (2). The lid carries a motor (3). Its shaft (5) also covered by Teflon is sealed with respect to the atmosphere. The conductance is measured by the conductivity cell (4). The lid is also provided with a port for filling the vessel (not shown).

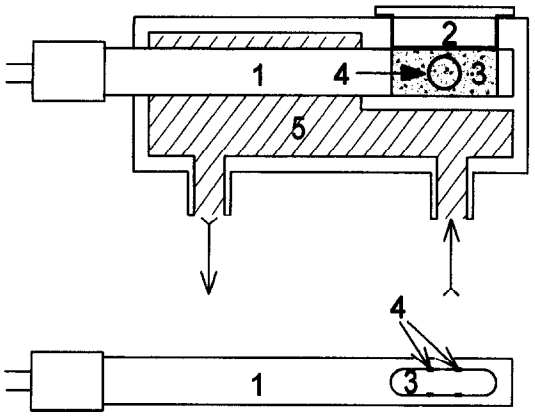


FIG. 4. Upper drawing: The conductivity cell (1) is surrounded by a cooling vessel (5) using thermostated water. The space (3) between the electrodes (4) is filled with sized calcite grains. After filling this space with a pre-equilibrated solution of $CO_2$, the set up is sealed by the lid (2). Lower drawing: The WTW-cell (1) showing the space (3) between the electrodes (4) in top view.

The electrodes (4) of the cell are located at the walls of a slit which is 3 cm long and 0.6 cm wide. This slit (3) is filled with 3 g of sized calcite. To start the experiment 2 $cm^3$ of a pre-equilibrated $CO_2$-$H_2O$ solution is filled into the calcite, and air bubbles in the porous medium are avoided by stirring for a few sec. The porous medium is covered with an airtight lid (2) to ensure closed-system conditions. This procedure takes less than 10 sec. To obtain dissolution rates the same electrode is used to measure the increase in conductivity. Each experiment was carried out three times. The results were reproduced within an error of 10%. To estimate the $V/A$-ratio from the average particle size we assume the particles as spheres with diameter $\bar{d}$ and simple cubic packing. Thus one obtains $V/A = 0.15 \cdot \bar{d}$ (Baumann et al., 1985). The corresponding porosity is 0.48.

## 4. RESULTS

The time course of the Ca-concentration for a batch experiment is depicted by Fig. 5. The solution approaches equilibrium closely within 10 min. The rates calculated from such curves are shown by Fig. 6a,b,c. The full dots represent the dissolution rates measured with a volume to surface area ratio $V/A = 0.60$ cm, the open squares are for experiments with $V/A = 0.038$ cm. The full lines A and B give the corresponding theoretical rates, calculated with the computer program of the theoretical model (Buhmann and Dreybrodt, 1985b; cf. also Fig. 2). The reduction of rates due to the increasing calcite surface is most pronounced for low $p_{CO_2}$, whereas for high pressures ($1 \cdot 10^{-1}$ atm) the concentration of $CO_2$ in the solution is sufficiently high to ensure sufficient $CO_2$-conversion for both $V/A$ ratios.

Figure 7 illustrates the evolution of the calcium concentration for the second type of experiments, where dissolution is active in a porous medium. The data in Fig. 7 were obtained from a run using marble with an average particle size of 150 $\mu$m. If the experimental rates follow a linear rate law (cf. Eqn. 3), then from Eqn. 4 one finds

$$c(t) = c_{eq}(1 - \exp(-t/\tau)) - c_{eq}, \tau = \frac{V}{A\alpha}. \quad (5)$$

The full line through the data points in Fig. 7 represents a fit of Eqn. 5 to the data. In all cases excellent fits to the data were obtained. This shows that a linear rate law is valid. There is, however, one important limitation. We have run all the experiments to concentrations very close to equilibrium. It was not possible to fit the whole time course with one exponential satisfactory. If, however, the data were truncated, omitting all data points with concentration $c > 0.9\ c_{eq}$ excellent fits were obtained in all cases. From these one obtains $\alpha$. This behaviour shows that close to equilibrium dissolution is inhibited and nonlinear rate laws are valid. This has already been suggested by Plummer and Wigley (1976), Palmer (1984, 1991), and Svensson and Dreybrodt (1992).

We have carried out such experiments at 5°, 10°, and 20°C, using Baker-calcite and sized material of marble. The values of $\alpha$ obtained from the fits are listed in Table 1 for two series of experiments with $p_{CO_2} = 5 \cdot 10^{-2}$ and $1 \cdot 10^{-2}$ atm. There is satisfactory agreement between the theoretically predicted kinetic constants $\alpha_{theo}$ and the experimental data $\alpha_{exp}$ with respect to both the temperature dependence and also the dependence on the $V/A$-ratio.

One should note that for Baker calcite with $V/A = 2.25 \cdot 10^{-4}$ cm $CO_2$-conversion is the rate limiting step in the process of dissolution. To give further evidence of this effect, we have performed an experiment, where the reaction $H_2O + CO_2 \rightarrow H^+ + HCO_3^-$ is accelerated by the enzyme carbonic anhydrase, which was added to the water with a concentration [E] of 0.6 $\mu$mole. From the Michaelis-Menten-equation the accelerated rate constant $k_{CO_2}^{acc}$ is obtained (Stryer, 1988) by

$$k_{CO_2}^{acc} = k_e \cdot [E]/(K_m + [CO_2]), \quad (6)$$

where $k_e$ is the turnover number of the enzyme and $K_m$ the Michaelis constant. Their values are $k_e = 6 \cdot 10^5 s^{-1}$ and $K_m = 8 \cdot 10^{-3}$ mole/litre at 25°C. We performed the experiment at 10°C and with an initial $p_{CO_2} = 5 \cdot 10^{-2}$ atm. In this run the $CO_2$-concentration drops from initially $1.6 \cdot 10^{-3}$ mole/litre to less than $1.6 \cdot 10^{-4}$ mole/litre, when equilibrium with respect to calcite is achieved. Therefore, $[CO_2]$ in the denominator of Eqn. 6 can be safely neglected. With [E] = 0.6 $\mu$mole/litre we obtain $k_{CO_2}^{acc} = 45\ s^{-1}$ which compared to the value $k_{CO_2} = 0.03\ s^{-1}$ is larger by a factor of 1500.

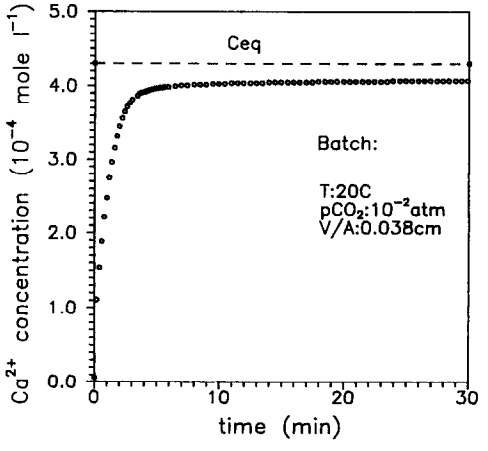


FIG. 5. Time course of a batch experiment. The equilibrium value $c_{eq}$ (dashed lines) is reached after 17 h.

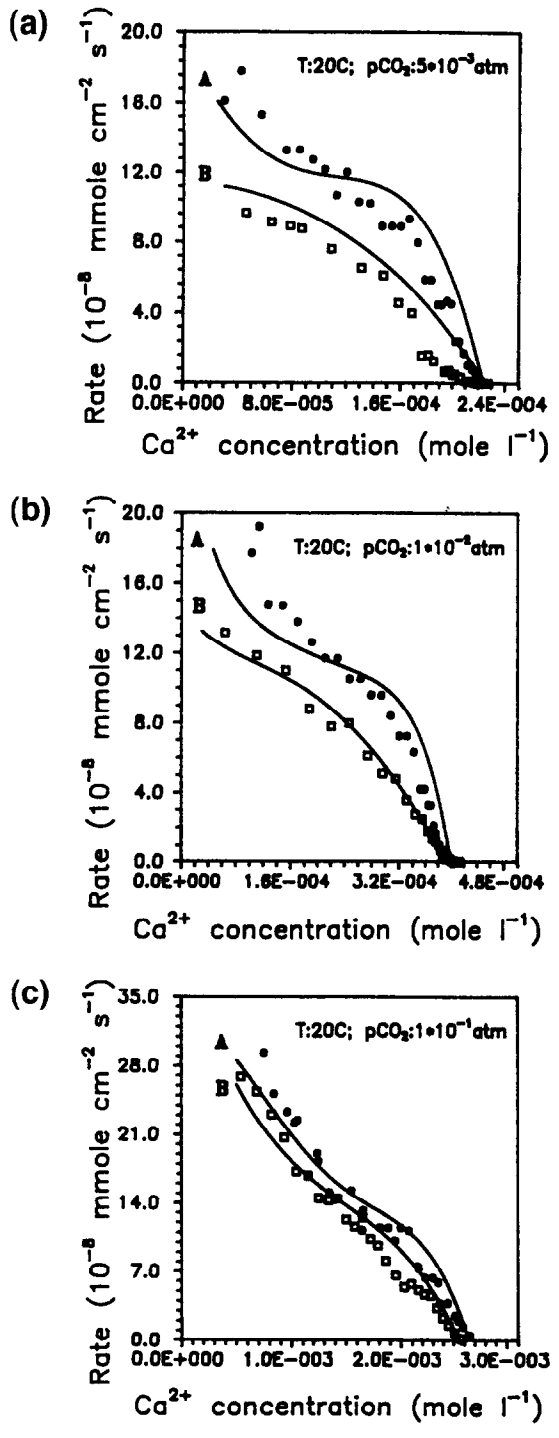


FIG. 6. Rates for free drift runs obtained from time courses as shown in Fig. 5. The upper curves (A) denote $V/A$ = 0.6 cm, the lower one (B) $V/A$ = 0.038 cm. The full lines are computed from the theoretical model. Note that with increasing $p_{CO_2}$ curves A and B approach each other.

Figure 8a shows the time course of the calcium concentration $c$ for the experiment using Baker calcite. In comparison to the analogous experiment without enzyme the reaction is drastically enhanced and the time $\tau$ = 100 s is reduced by a factor of about 50. In a second experiment we used sized marble with grain diameter between 700–1000 $\mu$m. Figure

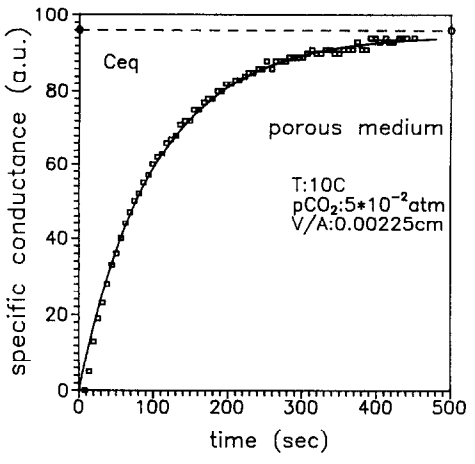


FIG. 7. Time course of an experiment using a porous medium of sized calcite grains. The equilibrium value is shown as dashed line. Units are arbitrary. Analysis of the porewater shows $c_{eq}$ = 2.12 mmole/l, i.e., close to saturation. The full line is a fit of Eqn. 5 to the experimental points ($\tau$ = 105 s, $c_{eq}$ = 96 a.u.).

8b shows the results. In this case, the enhancement is less pronounced and the time constant $\tau$ is reduced by a factor of three.

The value of $\alpha$ in both experiments employing carbonic anhydrase amounts to $\alpha_{CA} = 1 \cdot 10^{-4}$ cm s$^{-1}$ ($\pm$10%). This

**Table 1: Experimental values of $\alpha$ in comparison to the theoretical ones for various $V/A$-ratios.**

a) $p_{CO_2}$ = 5·10$^{-2}$ atm

| V/A [cm] | T°C | $\alpha_{exp}$ [cm s$^{-1}$] | $\alpha_{th}$ [cm s$^{-1}$] |
|---|---|---|---|
| 2.25·10$^{-4}$ | 5 | 1.5·10$^{-6}$ | 1.5·10$^{-6}$ |
| | 10 | 2.3·10$^{-6}$ | 2.7·10$^{-6}$ |
| | 20 | 6.4·10$^{-6}$ | 7.5·10$^{-6}$ |
| 2.25·10$^{-3}$ | 5 | 1.4·10$^{-5}$ | 1.3·10$^{-5}$ |
| | 10 | 2.3·10$^{-5}$ | 2.3·10$^{-5}$ |
| | 20 | 5.5·10$^{-5}$ | 5.3·10$^{-5}$ |
| 4.5·10$^{-3}$ | 5 | 1.1·10$^{-5}$ | 1.4·10$^{-5}$ |
| | 10 | 1.8·10$^{-5}$ | 2.4·10$^{-5}$ |
| | 20 | 4.7·10$^{-5}$ | 5.0·10$^{-5}$ |
| 6.8·10$^{-3}$ | 5 | 1.3·10$^{-5}$ | 1.5·10$^{-5}$ |
| | 10 | 1.8·10$^{-5}$ | 2.5·10$^{-5}$ |
| | 20 | 4.1·10$^{-5}$ | 4.9·10$^{-5}$ |
| 1.3·10$^{-2}$ | 5 | 1.0·10$^{-5}$ | 1.5·10$^{-5}$ |
| | 10 | 1.5·10$^{-5}$ | 2.4·10$^{-5}$ |
| | 20 | 4.0·10$^{-5}$ | 4.8·10$^{-5}$ |

b) $p_{CO_2}$ = 1·10$^{-2}$ atm

| V/A [cm] | T°C | $\alpha_{exp}$ [cm s$^{-1}$] | $\alpha_{th}$ [cm s$^{-1}$] |
|---|---|---|---|
| 2.25·10$^{-4}$ | 5 | 1.3·10$^{-6}$ | 1.3·10$^{-6}$ |
| | 10 | 2.0·10$^{-6}$ | 2.8·10$^{-6}$ |
| 1.6·10$^{-3}$ | 5 | 0.9·10$^{-5}$ | 1.0·10$^{-5}$ |
| | 10 | 1.9·10$^{-5}$ | 2.3·10$^{-5}$ |
| 4.5·10$^{-3}$ | 5 | 2.9·10$^{-5}$ | 2.8·10$^{-5}$ |
| | 10 | 5.1·10$^{-5}$ | 5.8·10$^{-5}$ |
| 6.8·10$^{-3}$ | 5 | 3.1·10$^{-5}$ | 3.8·10$^{-5}$ |
| | 10 | 4.5·10$^{-5}$ | 7.0·10$^{-5}$ |

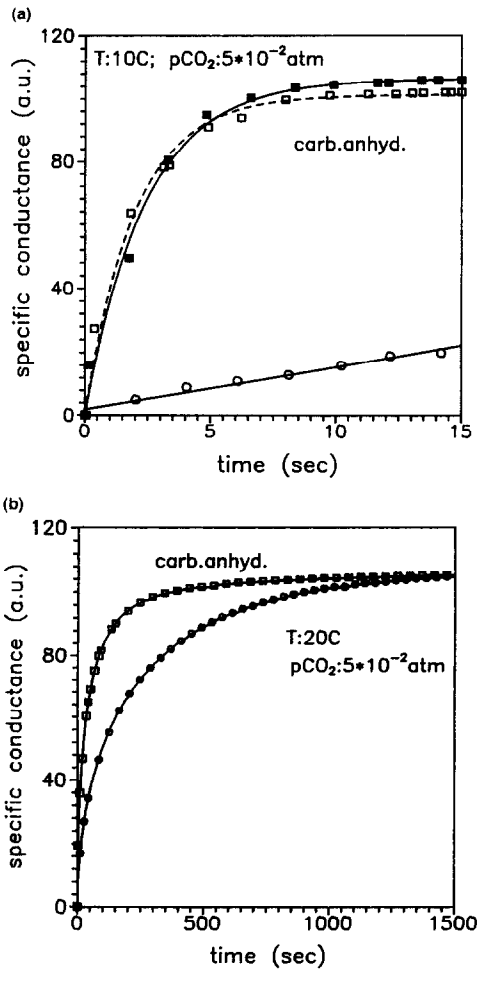


FIG. 8. Time course of the conductivity: (a) Baker calcite with carbonic anhydrase (0.6 $\mu$mol). The upper two curves show two different experiments. ($\bar{\tau}$ = 2.2 s). The lower curve gives the time course for the same experiment without carbonic anhydrase ($\bar{\tau}$ = 100 s). (b) The same experiment using marble with $\bar{d}$ = 850 $\mu$m.

is the value which is expected when surface reactions are rate limiting. For this case Buhmann and Dreybrodt (1985b) report a value of $\alpha = 1.5 \cdot 10^{-4}$ cm s$^{-1}$ at 10°C and $p_{CO_2}$ = 0.05 atm.

## 5. CONCLUSIONS

Some of the data from Table 1 are visualised in Fig. 9, where the rates calculated from Eqn. 3 are plotted by using the experimental data (full lines) and the theoretical ones (dashed lines). Although there are some deviations especially at higher values of the $V/A$-ratio, the general trend of the theory is well produced. At low $V/A$-ratios (Baker calcite, $V/A = 2.25 \cdot 10^{-4}$ cm), there is excellent agreement which shows clearly that $CO_2$-conversion is the rate limiting process. At $V/A = 2.25 \cdot 10^{-3}$ cm the rates have increased by a factor of 10 in agreement with the theoretical predictions. For $V/A = 4.5 \cdot 10^{-3}$ cm and $6.8 \cdot 10^{-3}$ cm the theory predicts little change in the values of $\alpha$. Even though the experimental data are higher by about 40% they exhibit a similar behaviour. Figure 10 gives an overview of the relation between the experimental and theoretical values of $\alpha$.

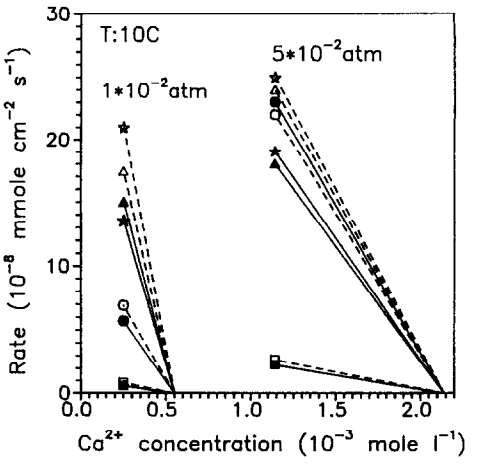


FIG. 9. Visualisation of some data from Table 1. The rates shown are calculated from Eqn. 3 using the experimental values (full lines) and the theoretical ones (dashed lines) of $\alpha$. The full and open symbols correspond to each other.

Here we have plotted $\alpha_{exp}$ vs. $\alpha_{th}$. The straight line through the data has a slope of 1.06 and results from a least square fit to the data. From this figure the good agreement of the experimental data to the theoretical ones becomes obvious. In spite of the uncertainty in the determination of the $V/A$ ratios from the average grain size diameter, and by a geometrical approximation assuming spheres this clearly demonstrates the validity of the theoretical model.

Good agreement between theory and experiment is also obtained for dissolution in the batch experiments (cf. Fig. 6a–c). Thus the experimental results give clear evidence of the reliability of the theoretical model of Buhmann and Dreybrodt (1985a,b). Although the experiments reported here have been performed at the condition of a system closed to $CO_2$, one can also infer the validity of the model for the open-system. The dissolution rates depend only on the chemical composition of the solution. Therefore, in a closed-system in equilibrium with given concentrations of $CO_2$ and $Ca^{2+}$ they are the same as in an open-system with an identical

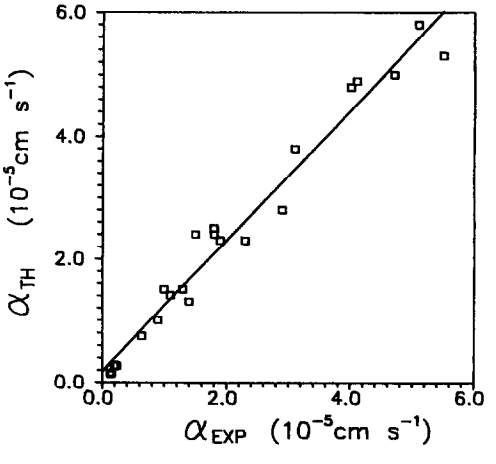


FIG. 10. Plot of $\alpha_{exp}$ vs. $\alpha_{th}$ for the experiments listed in Table 1. The full line is a least square fit to the data $\alpha_{th} = 1.06\ \alpha_{exp} + 0.18$.

chemical composition. Only the pathway along which this composition has been reached is different for both systems.

Thus the rates predicted from the theoretical model can be reliably used to estimate dissolution rates in many geological problems. There is one important restriction, however, which should be stressed here. As has been mentioned already in this paper, dissolution rates close to equilibrium are inhibited. Furthermore for $c \leq 0.2\ c_{eq}$ the theory of Buhmann and Dreybrodt (1985a,b) is not valid. In this region the reaction is limited by diffusion of $H^+$ to the surface, since the rate is determined by the term $\kappa_1(H^+)$ in Eqn. 2. The conclusions given here are, therefore, valid in the region $0.2\ c_{eq} \leq c \leq 0.9\ c_{eq}$.

*Acknowledgments*—One of us (L.Z.) gratefully acknowledges financial support of the University of Bremen.

*Editorial handling:* T. Paces

## REFERENCES

Baumann J., Buhmann D., Dreybrodt W., and Schulz W. (1985) Calcite dissolution kinetics in porous media. *Chem. Geol.* **53,** 219–228.

Buhmann D. and Dreybrodt W. (1985a) The kinetics of calcite dissolution and precipitation in geologically relevant situations of karst areas: 1. Open system. *Chem. Geol.* **48,** 189–211.

Buhmann D. and Dreybrodt W. (1985b) The kinetics of calcite dissolution and precipitation in geologically relevant situations of karst areas: 2. Closed system. *Chem. Geol.* **53,** 109–124.

Buhmann D. and Dreybrodt W. (1987) Calcite dissolution kinetics in the system $H_2O$-$CO_2$-$CaCO_3$ with participation of foreign ions. *Chem. Geol.* **64,** 89–102.

Dreybrodt W. (1987) The kinetics of calcite dissolution and its consequences to karst evolution from the initial to the mature state. *The NSS Bulletin* **49,** 31–49.

Dreybrodt W. (1988) Processes in karst systems—Physics, Chemistry and Geology. *Springer Ser. Phys. Environ.* **5.**

Dreybrodt W. (1990) The role of dissolution kinetics in the development of karstification in limestone: A model simulation of karst evolution. *J. Geol.* **98,** 639–655.

Dreybrodt W. (1992) Dynamics of Karstification: A Model applied to hydraulic structures in Karst Terranes. *Appl. Hydrogeol.* **1,** 20–32.

Dreybrodt W. and Buhmann D. (1991) A mass transfer model for dissolution and precipitation of calcite from solutions in turbulent motion. *Chem. Geol.* **90,** 107–122.

Dreybrodt W., Buhmann D., Michaelis J., and Usdowski, E. (1992) Geochemically controlled calcite precipitation by $CO_2$ outgassing: Field measurements of precipitation rates in comparison to theoretical predictions. *Chem. Geol.* **97,** 285–294.

Ford D. C. and Williams P. W. (1989) Karst geomorphology and hydrology. *Unwin Hyman.*

House W. A. and Howard J. R. (1984) Kinetics of Carbon Dioxide Transfer across the Air/Water Interface. Faraday Discuss. *Chem. Soc.* **77,** 33–46.

James A. N. (1992) Soluble Materials in Civil Engineering. Ellis Horwood Ser. Civil Eng. 434. Ellis Horwood.

Kern D. M. (1960) The hydration of carbon dioxide. *J. Chem. Educ.* **37,** 14–23.

Langmuir D. (1971) The geochemistry of some carbonate ground waters in Central Pennsylvania. *Geochim. Cosmochim. Acta* **35,** 1023–1045.

Liu Zaihua, Svensson U., Dreybrodt W., Yuan Daoxian, and Buhmann D. (1995) Hydrodynamic control of inorganic calcite precipitation in Huanglong Ravine, China: Field measurements and theoretical prediction of deposition rates. *Geochim. Cosmochim. Acta* **59,** 3087–3097.

Palmer A. N. (1984) Recent trends in karst geomorphology. *J. Geol. Educ.* **32,** 247–253.

Palmer A. N. (1988) Solutional enlargement of opening in the vicinity of hydraulic structures in karst regions. *Assoc. Groundwater Sci. Eng., 2nd Conf. Environ. Problems Karst Terranes and their Solutions, Proc.* 3–15.

Palmer A. N. (1991) The origin and morphology of limestone caves. *Geol. Soc. America Bull.* **103,** 1–21.

Plummer L. N. and Wigley T. L. M. (1976) The dissolution of calcite in $CO_2$-saturated solutions at 25°C and 1 atm total pressure. *Geochim. Cosmochim. Acta* **40,** 1991–2002.

Plummer L. N., Wigley T. L. M., and Parkhurst D. L. (1978) The kinetics of calcite dissolution in $CO_2$-water systems at 5°C to 60°C and 0.0 to 1.0 atm. $CO_2$. *Amer. J. Sci.* **278,** 537–573.

Schulz H. D. (1988) Labormessung der Sättigungslänge als Maß für die Lösungskinetik von Karbonaten im Grundwasser. *Geochim. Cosmochim. Acta* **52,** 2651–2657.

Stryer L. (1988) *Biochemistry.* W. H. Freeman and Co.

Stumm W. and Morgan J. J. (1981) *Aquatic Chemistry, An Introduction Emphasizing Chemical Equilibria in Natural Waters.* Wiley.

Svensson U. and Dreybrodt W. (1992) Dissolution kinetics of natural calcite minerals in $CO_2$-water systems approaching calcite equilibrium. *Chem. Geol.* **100,** 129–145.

Trudgill S. T. (1985) *Limestone Geomorphology.* Longman.

Usdowski E. (1982) Reactions and equilibria in the systems $CO_2$-$H_2O$ and $CaCO_3$-$CO_2$-$H_2O$. A review. *Neues Jahrb. Mineral. Abh.* **144,** 148–171.

White W. B. (1988) *Geomorphology and Hydrology of Karst Terrains.* Oxford Univ. Press.